

Ivantsov parabolic solution for two combined moving interfaces

D. Temkin

Institut für Festkörperforschung, Forschungszentrum Jülich,
D-52425 Jülich, Germany

Contact e-mail: d.temkin@gmx.de

September 13, 2021

Abstract

We demonstrate that for a migration of a liquid layer between the melting and the solidification front an exact steady-state solution with two parabolic fronts can be found. A necessary condition hereby is that the temperature of the solidification front exceeds the temperature of the melting front (both temperatures are supposed to be constant). It is shown that in pure materials and alloys there exist two types of solutions with two convex and with two concave parabolas respectively. While a steady-state process with two planar interfaces is only possible for a single point, the processes with two parabolas are possible inside a region of control parameters. The relations between the Peclet numbers and the control parameters are obtained.

1 Introduction

Liquid film migration (LFM) is well-known phenomenon which has been observed in many alloy systems during sintering in the presence of liquid phase [1, 2] and in Cu-In solid solutions during melting started at grain boundaries [3]. In LFM, one of crystals is melted and the other one is solidified. The both solid-liquid interfaces are moving together with the same velocity. In the investigated alloys systems the migration velocity is of the order of $10^{-8} - 10^{-7} \text{ m} \cdot \text{s}^{-1}$ and it is controlled by the solute diffusion through a thin liquid layer between the two interfaces [4]. The migration velocity is much smaller than the characteristic velocity of atomic kinetics at the interfaces. Therefore the both solids at the interfaces must be at the local thermodynamic equilibrium with liquid. The theory [4] answers the question about the different equilibrium states at the melting and solidification fronts. In a steady-state regime, the difference in equilibrium relates to coherency stresses appearing only at the melting front due to the sharp profile of composition ahead the moving melting front. Thus, the liquid composition at the melting front which depends on the coherency strains and a curvature of the front differs from the liquid composition at unstressed and curved solidification front. The migration velocity is proportional to the difference of these compositions divided by the film thickness [4]. But what controls the thickness?

Consequently, a new problem of two combined moving solid-liquid interfaces with a liquid between them appears. In the present article, this problem is considered under simplified boundary conditions: the temperature and chemical composition along each interface are constant. These constants are different for the melting and solidification fronts and differ from those far from the migrating liquid film. It means that any capillary, kinetic and crystallographic effects at the interfaces are neglected. It is found that under these simplified boundary conditions two co-focal parabolic fronts can move together with the same velocity. The situation is rather similar to a steady-state motion of one parabolic solidification front

into a supercooled melt [5, 6] or one parabolic melting front into a superheated solid.

2 Solutions for one parabolic front

Needle-like stationary solutions were first obtained by Ivantsov for the crystallization of a pure material from a supercooled melt [5] and were extended to binary alloys [6]. This solution describes a parabolic interface of a solid phase at constant temperature T_m which extends into a supercooled melt. Inside the melt the temperature drops and reaches far from the interface its asymptotic value $T_0 < T_m$.

For the two-dimensional case the Ivantsov relation is

$$\Delta = F(P) \equiv \sqrt{\pi P} e^P \operatorname{erfc}(\sqrt{P}) \quad , \quad 0 \leq \Delta < 1. \quad (1)$$

It connects the Peclet number $P = VR/2D$ and the supercooling $\Delta = (T_m - T_0)c/q$. Here V and R are the front-velocity and the tip-radius of the parabola respectively; D and c are the thermal diffusivity and the specific heat of the melt, respectively, q is the latent heat.

Eq. (1) can easily be obtained in 2D-parabolic coordinates (η, ξ) (see, for example, Ref. [7])

$$\begin{aligned} \eta &= \sqrt{x^2 + z'^2} + z' \quad , \quad \xi = \sqrt{x^2 + z'^2} - z' \quad , \quad 0 \leq (\eta, \xi) < \infty, \\ x &= \pm\sqrt{\eta\xi} \quad , \quad z' = \frac{1}{2}(\eta - \xi) \quad , \quad -\infty < (x, z') < \infty, \end{aligned} \quad (2)$$

where $(x, z' = z - Vt, t)$ are the Cartesian coordinates and the t is the time. In this description the parabolic solidification front ($z' = \frac{R}{2} - \frac{x^2}{2R}$), moving with velocity V in the positive z -direction, has the coordinate $\eta = R$. The regions $0 \leq \eta < R$ and $R < \eta < \infty$ correspond to the solid and the liquid phase respectively.

In this set of coordinates, the temperature field T in both phases depends only on η . The

thermal diffusion equation

$$\frac{\partial}{\partial \eta} \left(\sqrt{\eta} \frac{\partial T}{\partial \eta} \right) + \frac{V}{2D} \left(\sqrt{\eta} \frac{\partial T}{\partial \eta} \right) = 0 \quad (3)$$

is easily solved by the ansatz

$$T(\eta) = A + B \int \eta^{-1/2} e^{-V\eta/2D} d\eta \quad (4)$$

with different constants A and B for the solid and the liquid phase. These constants and Eq. (1) can be obtained by using the appropriate boundary conditions, namely the asymptotic boundary condition $T(\eta \rightarrow \infty) = T_0$ and the interfacial conditions of temperature continuity $T(R-0) = T(R+0) = T_m$, and heat balance at the interface

$$Vq/c = -2DT'(R+0) + 2DT'(R-0), \quad (5)$$

where the prime denotes the derivative with respect to η . For reasons of simplicity we assumed the same values for D and c in both phases.

Apart from the solution with convex parabolic front there exists as well a solution with a concave front ($z' = -\frac{R}{2} + \frac{x^2}{2R}$). In the parabolic coordinates, the interface is defined by the relation $\xi = R$ while solid and liquid phase are at $\infty < \xi < R$ and $R > \xi \geq 0$, respectively. In contrast to the former case the temperature field T depends only on ξ . Instead of Eq. (3) the diffusion equation therefore reduces to

$$\frac{\partial}{\partial \xi} \left(\sqrt{\xi} \frac{\partial T}{\partial \xi} \right) - \frac{V}{2D} \left(\sqrt{\xi} \frac{\partial T}{\partial \xi} \right) = 0 \quad , \quad (6)$$

and is solved by the ansatz

$$T(\xi) = A + B \int \xi^{-1/2} e^{V\xi/2D} d\xi \quad . \quad (7)$$

While the conditions of continuity and heat balance at the interface stay the same as for the convex parabola, the asymptotic condition changes to $T(\xi \rightarrow 0) = T_0$. Thus for the concave

front instead of Eq. (1) we obtain the relation

$$\Delta = \Phi(P) \equiv 2\sqrt{P} e^{-P} \int_0^{\sqrt{P}} e^{x^2} dx \quad 0 \leq \Delta \leq 1.284\dots , \quad (8)$$

between the supercooling Δ and the Peclet number P . The function $\Phi(P)$, in contrast to the function $F(P)$ in Eq. (1), is not monotonous: it has a maximum $1.284\dots$ at $P = 2.25\dots$ and approaches 1 from above for $P \rightarrow \infty$.

Naturally, Eq. (1) and Eq. (8) describe as well a parabolic melting front: the superheated solid phase with $T_0 > T_m$ is outside the convex parabola ($\eta = R$) at $R < \eta < \infty$ or inside the concave one ($\xi = R$) at $R > \xi \geq 0$. The melting heat is $-q$.

3 Two parabolic fronts in a pure material

It turns out, that an exact steady-state solution with a combined motion of the two co-focal parabolic fronts (melting and solidification front with a liquid layer in between) can be found. For this the solidification front temperature T_m has to exceed the temperature \tilde{T}_m on the melting front. This may be the case for pure materials where the melted solid phase (S1) has with respect to the solidified solid (S2) an additional contribution ϵ to the energy-density (for example due to preliminary mechanical treatment). In this case the melting heat equal to $-(q - \epsilon)$ and the melting temperature $\tilde{T}_m = T_m(1 - \epsilon/q)$ differ from the values q and T_m for the solidification front. The additional energy ϵ is the driving force for a recrystallization process, which takes place in the solid either due to a migration of a boundary between a S1- and a S2-grain or due to a possible recrystallization through a liquid layer between S1 and S2.

It should be pointed out, that a combined stationary motion of two planar interfaces (with equilibrium temperatures T_m and \tilde{T}_m) is only possible at the temperature $T_{0,0}$ at which the temperature increase $(T_m - T_{0,0})$ exactly compensates the additional energy, $c(T_m - T_{0,0}) = \epsilon$.

All temperatures deviating from $T_{0,0}$ lead to an increase (at $T_0 > T_{0,0}$) or to a decrease and disappearance (at $T_0 < T_{0,0}$) of the liquid layer between the planar interfaces. Here only two co-focal parabolic interfaces can lead to a steady-state motion.

Similar to the considerations described for one interface an analysis of the temperature field in parabolic coordinates leads to the following relations:

For two convex parabolas with $P_1 > P_2$ (Fig. 1):

$$\Delta_m = 2\sqrt{P_2}e^{P_2} \int_{\sqrt{P_2}}^{\sqrt{P_1}} e^{-x^2} dx \quad (9)$$

$$\Delta = \left[1 - \alpha\Delta_m - \sqrt{\frac{P_2}{P_1}} e^{P_2-P_1} \right] F(P_1). \quad (10)$$

For two concave parabolas with $P_1 < P_2$ (Fig. 1):

$$\Delta_m = 2\sqrt{P_2}e^{-P_2} \int_{\sqrt{P_1}}^{\sqrt{P_2}} e^{x^2} dx, \quad (11)$$

$$\Delta = \left[1 - \alpha\Delta_m - \sqrt{\frac{P_2}{P_1}} e^{P_1-P_2} \right] \Phi(P_1), \quad (12)$$

with $P_i = VR_i/2D$, $\Delta_m = (T_m - \tilde{T}_m)c/q$, $\Delta = (T_0 - \tilde{T}_m)c/q$ and $F(P)$ and $\Phi(P)$ as in Eq. (1) and Eq.(8). $\alpha = q/cT_m$ is a material parameter (e.g., for Ni one has $\alpha \cong 0, 25$). The term $(1 - \alpha\Delta_m)$ arises due to the fact that the melting heat of a solid phase S1 with an additional energy density ϵ differs from the equilibrium melting heat, $-q$ (note that $-(q - \epsilon) = -q(1 - \alpha\Delta_m)$).

In the corresponding limiting cases Eqs. (9)-(12) reduce to Eqs. (1) and (8): Eq. (9) for $P_1 \rightarrow \infty$ and Eq. (11) for $P_1 \rightarrow 0$ lead to the solidification relations Eq. (1) and Eq. (8), respectively, with supercooling Δ_m instead of Δ . Eq. (10) for $P_2 \rightarrow 0$ and Eq. (12) for $P_2 \rightarrow \infty$ lead to the melting relations Eq. (1) and Eq. (8) with the normalized superheating $\Delta/(1 - \alpha\Delta_m)$ instead of Δ .

4 Analysis of convex and concave solutions

Even if Eqs. (9) - (12) are valid for arbitrary values of the normalized driving force $\Delta_m > 0$, we consider in the following analysis the case of small driving forces $\Delta_m \ll 1$. With this assumption Eqs. (9) and (11), respectively, simplify to

$$\sqrt{P_2} \cong \frac{1}{2} \left[\sqrt{P_1} \pm \sqrt{P_1 - 2\Delta_m} \right] \quad (P_1 > P_2) \quad (13)$$

$$\sqrt{P_2} \cong \frac{1}{2} \left[\sqrt{P_1} + \sqrt{P_1 + 2\Delta_m} \right] \quad (P_1 < P_2). \quad (14)$$

Eq. (13) together with Eq. (10) and Eq. (14) together with Eq. (12) define for the case of small driving forces $\Delta_m \ll 1$ the dependency of $\Delta(P_1)$ for both types of solutions (concave and convex parabolas) (see Fig. 2).

For $P_1 \gg \Delta_m$ the upper branch of Eq. (13) gives

$$P_2 \cong P_1 - \Delta_m \quad (P_1 > P_2) \quad (15)$$

and from Eq. (14)

$$P_2 \cong P_1 + \Delta_m \quad (P_1 < P_2). \quad (16)$$

Using this simplification and taking the limit $\Delta_m \rightarrow 0$ we obtain from Eqs. (10) and (12) the simplified expressions

$$\frac{\Delta}{\Delta_m} = \left(1 - \alpha + \frac{1}{2P_1}\right) F(P_1) \quad , \quad (P_1 > P_2) \quad , \quad (17)$$

$$\frac{\Delta}{\Delta_m} = \left(1 - \alpha - \frac{1}{2P_1}\right) \Phi(P_1) \quad , \quad (P_1 < P_2) \quad . \quad (18)$$

A stationary solution with two convex parabolas ($P_1 > P_2$) exists for

$$\Delta_0 \leq \Delta \leq \Delta^* \quad (19)$$

with

$$\Delta_0 \equiv (1 - \alpha) \Delta_m \quad \text{and} \quad \Delta^* \equiv 1 - \alpha \Delta_m. \quad (20)$$

The point $\Delta = \Delta_0$ corresponds to the steady-state solution of two moving planar interfaces mentioned above.

If $\Delta_0 \leq \Delta \ll \Delta_1$, the dependence of Δ on P_1 is defined by Eq. (17) and $P_2 \cong P_1 - \Delta_m$. At the point $\Delta = \Delta_1 \cong \sqrt{\pi\Delta_m/2}$ one has $P_1 \cong 2\Delta_m$ and $P_2 \cong \Delta_m/2$. In the vicinity of the Δ_1 -point one can obtain

$$\frac{\Delta - \Delta_1}{\Delta_1} \cong \mp \sqrt{\frac{P_1}{2\Delta_m} - 1}. \quad (21)$$

From Eqs. (9) and (10), one can obtain that close to the limiting point Δ^* one gets

$$P_1 \cong \frac{\Delta^*}{2(\Delta^* - \Delta)} \gg 1 \quad \text{and} \quad P_2 \cong \frac{\Delta_m^2}{\pi} \ll 1. \quad (22)$$

These relations describe the independent motion of both parabolic fronts propagating with the same velocity.

Solutions of Eqs. (12) - (14) for a pair of concave parabolas exist in the region

$$- |\Delta_4| \leq \Delta \leq \Delta_2 \quad (23)$$

between two extreme points on the $\Delta(P_1)$ -dependence (Fig. 2): minimum point $|\Delta_4| \cong \Delta_m$ at $P_1 \cong \sqrt{\Delta_m/4(1-\alpha)}$ and maximum point Δ_2 which is close to Δ_0 . In the limit $P_1 \rightarrow \infty$ the value of Δ tends to the same point Δ_0 as for the convex parabolas, $\Delta \cong \Delta_0 - \alpha/2P_1$.

5 Parabolic solutions for binary alloys

Extending our analysis to a two-component alloy, we have to take into account that in contrast to a pure material the temperatures T_1 and T_2 of the melting and solidification fronts are unknown (in a pure material $T_1 = \tilde{T}_m$, $T_2 = T_m$). In order to define T_1 and T_2 (and consequently $\Delta_m = (T_2 - T_1)c/q$, and $\Delta = (T_0 - T_1)c/q$ in Eqs. (9)-(12)) we have to obtain two additional equations.

In our description, we denote the molar fraction of the second component with C and the diffusion coefficients in the solid and the liquid phase with D_S and D_L respectively. While for convex parabolas the concentration fields, $C(\eta, \xi)$, only depend on η , they depend only on ξ in the concave case. In the first case, the field $C(\eta)$ satisfies the equilibrium boundary conditions at both interfaces, namely the continuity condition

$$C(R_2 - 0) = C_S(T_2) , \quad C(R_2 + 0) = C_L(T_2) , \quad C(R_1 - 0) = \tilde{C}_L(T_1) , \quad C(R_1 + 0) = \tilde{C}_S(T_1) , \quad (24)$$

the far field condition $C(\eta \rightarrow \infty) = C_0$ and the conservation conditions at the interfaces

$$V [C_L(T_2) - C_S(T_2)] = -2D_L C'(R_2 + 0) + 2D_S C'(R_2 - 0) , \quad (25)$$

$$V [\tilde{C}_L(T_1) - \tilde{C}_S(T_1)] = -2D_L C'(R_1 - 0) + 2D_S C'(R_1 + 0) . \quad (26)$$

Here $C_S(T_2)$ and $C_L(T_2)$ are the solidus and liquidus compositions which are defined by the equilibrium phase diagram of the alloy, while $\tilde{C}_S(T_1)$, $\tilde{C}_L(T_1)$ are the corresponding values defined by a disturbed phase diagram. The additional energy density ϵ , changing the melting point of the melted solid phase S1, will change the equilibrium compositions at the melting interface as well. In this case, the composition differences $\tilde{C}_S(T_1) - C_S(T_1)$, $\tilde{C}_L(T_1) - C_L(T_1)$, are proportional to ϵ/q . Another reason for the distortion of the phase diagram are coherency stresses due to compositional inhomogeneities in front of the melting interface [4].

By solving the diffusion equation for $C(\eta)$ and applying the appropriate boundary conditions (24)-(26), we obtain for the case of convex parabolas the solution:

$$\frac{C_L(T_2) - \tilde{C}_L(T_1)}{C_L(T_2) - C_S(T_2)} = 2\sqrt{P_{2L}} e^{P_{2L}} \int_{\sqrt{P_{2L}}}^{\sqrt{P_{1L}}} e^{-x^2} dx , \quad P_{1L} > P_{2L} \quad (27)$$

$$\frac{C_0 - \tilde{C}_S(T_1)}{C_L(T_2) - C_S(T_2)} = \left[\frac{\tilde{C}_L(T_1) - \tilde{C}_S(T_1)}{C_L(T_2) - C_S(T_2)} - \sqrt{\frac{P_{2L}}{P_{1L}}} e^{P_{2L} - P_{1L}} \right] F(P_{1S}) \quad (28)$$

$(P_{iL} = DP_i/D_L, P_{1S} = D_L P_{1L}/D_S; F(P)$ is the same function as in Eq. (1)). A similar consideration for the case of concave parabolas with concentration field $C(\xi)$ leads to:

$$\frac{C_L(T_2) - \tilde{C}_L(T_1)}{C_L(T_2) - C_s(T_2)} = 2\sqrt{P_{2L}} e^{-P_{2L}} \int_{\sqrt{P_{1L}}}^{\sqrt{P_{2L}}} e^{x^2} dx , \quad P_{1L} < P_{2L} \quad (29)$$

$$\frac{C_0 - \tilde{C}_s(T_1)}{C_L(T_2) - C_s(T_2)} = \left[\frac{\tilde{C}_L(T_1) - \tilde{C}_s(T_1)}{C_L(T_2) - C_s(T_2)} - \sqrt{\frac{P_{2L}}{P_{1L}}} e^{P_{1L} - P_{2L}} \right] \Phi(P_{1S}), \quad (30)$$

where $\Phi(P)$ is defined by the same manner as in Eq. (8).

For the convex configuration, Eqs. (9)-(10) together with Eqs. (27)-(28) describe the dependency of the quantities T_1, T_2, P_1, P_2 on the initial control parameters T_0, C_0 , and ϵ . The corresponding relations for the concave configuration are given by Eqs. (11)-(12) and Eqs. (29)-(30). In systems with vanishing ϵ the coherency strain effect can support the combined motion of two interfaces as, for example, in liquid film migration [4].

6 Discussion

The considered two fronts process (TFP) is an alternative to an one front process (OFP). TFP is possible at some conditions (for example, at $\tilde{T}_m < T_m$ for a pure material) and do exist as a steady-state process in a definite region of control parameters. In this region there is one or a few OFP. For pure materials the TFP exists at $-|\Delta_4| \leq \Delta \leq \Delta^*$ (see Eqs. (19) and (23)), i.e. at $\tilde{T}_m - (T_m - \tilde{T}_m) \leq T_0 \leq \tilde{T}_m + (q - \epsilon)/c$. When the initial temperature is $T_0 < \tilde{T}_m < T_m$, the OFP of the transition $S1 \rightarrow S2$ proceeds at the grain boundary $S1/S2$. When $\tilde{T}_m < T_0 < T_m$, the OFP of the melting of $S1$ at the interface $S1/L$ is also possible. At $T_0 > T_m$ the grain $S2$ can also be melted at the interface $S2/L$. The TFP can proceed faster than the corresponding OFP due to a heat transfer between melting and solidification fronts through a thin liquid layer. In order to initiate the TFP (especially at $\tilde{T}_m - (T_m - \tilde{T}_m) \leq T_0 \leq \tilde{T}_m$) a liquid phase must be created inside the system. Then the

grain boundary $S1/S2$ splits into two interfaces, $S1/L$ and $S2/L$, and the TFP proceeds as a self-sustained process.

It should be noted that the TFP can take place in a pure material in which there are several polymorphic modifications. Then a low temperature modification plays a role of the melted grain $S1$ in Fig. 1 and its melting temperature \tilde{T}_m is lower than the melting temperature T_m for a high temperature modification, $S2$. In such a case the solutions given by Eqs. (9) - (12) are valid for $\Delta_m = (T_m - \tilde{T}_m)c/q$ as a material parameter and $(1 - \alpha\Delta_m)$ is replaced by another material parameter \tilde{q}/q , where \tilde{q} and q are the melting heats of the low and high temperature phases respectively.

Generally, one can consider the TFP of the transition of a phase $S1$ into another phase $S2$ through an intermediate phase L (which is not necessarily a liquid one) as an alternative to the OFP of the direct transition $S1 \rightarrow S2$.

The obtained Eqs. (9) - (12) together with Eqs. (27) - (30), which define relations between the Peclet numbers P_1 , P_2 and control parameters T_0 , C_0 , give the continuous spectrum of solutions with the only free parameter (e.g., the velocity V). Therefore an additional equations, i.e. “selection” relationship, is needed in order to define the unique solution. This is similar to a well-known “selection” problem in dendritic growth [8]. A search for the selection condition will be a subject of future investigation. The only point which might be stressed here is the following.

The structure of the fronts is usually more complicated compared to pure parabolic ones due to possible cellular structures or due to finite size of the sample. In this case, two parabolas describe only a part of the moving fronts. The complete shape of the fronts must be subjected to additional boundary conditions. One can speculate on possible cellular structures with two moving interfaces which are shown in Fig. 3. These structures should appear due to the diffusional interaction between different cells and capillary effects play

also crucial role. The structures have central parabolic parts which are convex (Fig. 3(a,b)) or concave (Fig. 3(c)) and satisfy boundary conditions of zero heat- and mass-fluxes across boundaries of cells. The first structure (Fig. 3(a)) can be related to a melting processes and the other two ones, for example, to sintering of two solid grains $S1$ and $S2$ in liquid phase L . The structure in Fig. 3(b) may correspond to a sintering process with a supersaturated solid $S1$, while the structure in Fig. 3(c) with a concave central part may correspond to the case of undersaturated solid $S1$.

In the process in the channel (or cell) the fronts velocity may be controlled either by the above mentioned cell boundary conditions or by the “selection” which takes place mostly in the parabolic region. Such a problem arises also in the selection of the growth velocity of the classical dendrite in the channel (the structure with one front) [8].

In this paper the solutions are obtained for two parabolic fronts in the two dimensions. Similar solutions can be easily found for two paraboloidal interfaces in the three dimensions.

A few words about the solutions (1) and (8) for one convex and one concave parabolic interface might be outlined. The convex parabola and Eq. (1) are playing an important role in dendritic solidification (see, e.g., Ref. [8]) and must be important in “dendritic” melting. It can be supposed that concave parabola and Eq. (8) are playing a role in such “doublon” structures with two convex parts and a concave part in between which are similar to the profile of $S2/L$ -interface in Fig. 3(c). Whether or not those “doublon” structures exist in solidification or melting processes with one front?

7 Conclusions

A theoretical model for combined motion of two solid-liquid fronts with a liquid layer in between has been developed for pure materials and binary alloys. The temperature and

chemical compositions at the interfaces were supposed to be constants but different for fronts of melting and solidification.

An exact solution which describes the steady-state motion of two co-focal parabolic interfaces has been found. It is shown that there exist two types of solutions with two convex and with two concave parabolas. The relations between the Peclet numbers and the control parameters of the process for both types of solutions are obtained.

As usual in theories of the steady-state growth, the continuous spectrum of solutions with one free parameter exists. The unresolved problem of “selection” of unique solution is briefly discussed.

8 Acknowledgments

This work was supported in part by the Deutsche Forschungsgemeinschaft under project SPP 1120. The author would like to thank L. Bagrova, E. Brener, P. Galenko, and H. Müller-Krumbhaar for fruitful discussions.

References

- [1] Yoon DN, Hupmann WJ. *Acta Metall* 1979;27:973.
- [2] Yoon DN. *Int Mater Rev* 1995;40:149.
- [3] Muschik T, Kaysser WA and Hohenkamp T. *Acta Metall* 1989;37:603.
- [4] Yoon DN, Cahn JW, Handwerker CA, Blendell JE, Baik YJ. In: *Interface Migration and Control of Microstrucutres*. Am Soc. Metals. Park. Ohio (1985), pp. 19-31.
- [5] Ivantsov GP. *Dokl Akad Nauk SSSR* 1947;58:567.
- [6] Ivantsov GP. *Dokl Akad Nauk SSSR* 1952;83:573.
- [7] Saito Y. *Statistical Physics of Crystal Growth*, World Scientific Publishing, Singapore, 1996.
- [8] Brener EA, Mel'nikov VI. *Adv Phys* 1991;40:53.

FIGURE CAPTIONS

Figure 1: Two types of combined moving parabolic fronts: convex (left) and concave (right).

Figure 2: The dependence of the reduced temperature Δ on the Peclet number P_1 for convex and concave fronts. The insert represents the region of small Δ . Parameters are: $\Delta_m = 0.01$ and $\alpha = 0.25$.

Figure 3: Three possible cellular structures of two combined moving interfaces with convex [(a) and (b)] and concave (c) central parabolic part. $S1$ and $S2$ are melting solid and growing solid, and L is the liquid phase. The direction of motion is defined by the arrow of V . Dashed regions in (a)-(c) show the central parabolic part of interfaces.

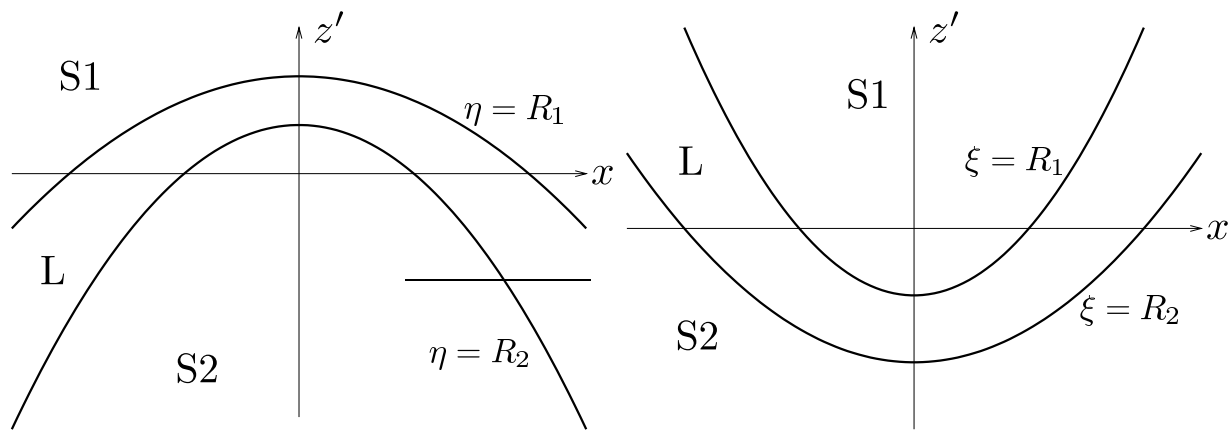


Figure 1:

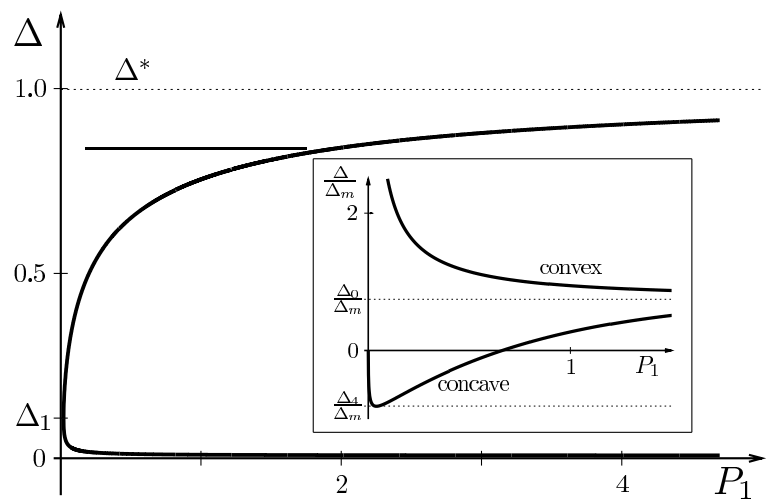


Figure 2:

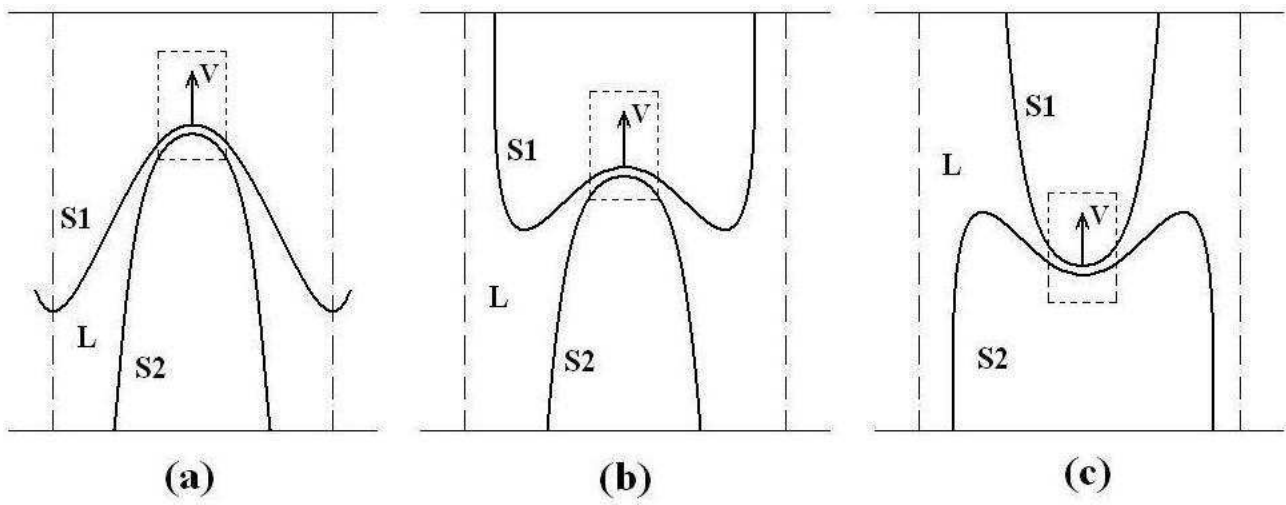


Figure 3: